RESEARCH ARTICLE

INTERNATIONAL RESEARCH JOURNAL OF MULTIDISCIPLINARY TECHNOVATION

Asian Research Association

DOI: 10.54392/irjmt2549

Design and Control of a Dual Inverter-Based Grid-Tied PV System with QB Converter: Comparison of PI and FOPID Controller Performance

Shaik Masum Basha [a, *], K. Nagaraju [b]

[a] Department of Electrical and Electronics Engineering, JNTUA-Ananthapuramu, India
[b] Department of Electrical and Electronics Engineering, PVKK Institute of Technology, Ananthapuramu, India
* Corresponding Author Email: smasumbasha@gmail.com

DOI: https://doi.org/10.54392/irjmt2549
Received: 27-01-2025; Revised: 05-06-2025; Accepted: 17-06-2025; Published: 15-07-2025

Abstract: This paper presents the design and implementation of a dual inverter-based grid-connected photovoltaic (PV) system incorporating PI (Proportional-Integral) and FOPID (Fractional-Order Proportional-Integral-Derivative) controllers, along with a Quadratic Boost Converter (QBC) for enhanced energy conversion and grid integration. In order to guarantee optimal DC-AC conversion from the photovoltaic array and smooth grid integration, the dual inverter system features cascaded voltage source two level inverters (DI). Enhancing power quality, improving the system's dynamic response, and making sure the injected current satisfies the necessary requirements while lowering harmonic content are the main goals. While the FOPID controller is used to enhance the system's transient response and provide better dynamic performance under changing irradiance and grid disturbances, the PI controller is employed for steady-state control. The Quadratic Boost Converter is a great option for PV applications since it also has a high efficiency, a high step-up voltage conversion, and lower switching losses. The FOPID controller reduces settling time by 43% and overshoot for grid current by 38% when compared to the PI controller, according to a comparative study of the two controllers. Furthermore, the grid current's Total Harmonic Distortion (THD) is decreased from 4.41% (PI) to 4% (FOPID). These outcomes demonstrate how well the twin inverter-based PV system with the QBC works and how the FOPID controller provides better dynamic performance for grid-tied applications.

Keywords: Photovoltaic Panels, Cascaded Voltage Source Two Level Inverter (DI), PI, FOPID, Harmonic Distortion, SVPWM, QBC.

1. Introduction

The growing need for clean, sustainable energy sources and the global need to cut greenhouse gas emissions have fueled the explosive growth of renewable energy technology, especially photovoltaic (PV) systems [1, 2]. In order to effectively incorporate solar energy into traditional power networks and facilitate real-time energy exchange with the utility grid, grid-tied PV systems have become a crucial solution [3]. However, when interfaced with intricate power electronic converters, these systems frequently experience operational difficulties pertaining to voltage mismatch, power quality, and control stability [4, 5]. As solar energy penetration increases, the grid integration challenges become more pronounced, requiring advanced control and conversion techniques to maintain system reliability and power quality [6, 7].Researchers have looked into several power converter layouts and control strategies to improve the performance of PV systems [8, 9]. Among these, the quadratic boost converter (QBC) [8] has drawn interest because it can provide a larger voltage gain than traditional boost converters, which is especially useful in situations when the PV voltage is low or varies because of external factors [10, 11]. Furthermore, QBCs are particularly advantageous in low-voltage PV applications, where maintaining a high conversion efficiency with minimal ripple is essential for downstream inverter performance [12, 13].High voltage gain and bidirectional power flow can be achieved by integrating a QBC with a dual inverter construction, which would enable smooth energy exchange with the grid [14]. Along with topological enhancements, grid-tied PV systems' dynamic control is still a primary priority. Despite being straightforward and extensively used, traditional proportional-integral (PI) controllers [15, 16] frequently perform poorly when non-linearities and fluctuating operating circumstances are present. They lack robustness in fast-changing conditions such as partial shading, load variation, or grid faults [17]. As a more sophisticated option, Fractional Order Proportional-Integral-Derivative (FOPID) controllers

increase system stability and dynamic response by providing more degrees of freedom through its fractional calculus formulation. The key objectives of this study are: To design and simulate a dual inverter-based grid-tied PV system integrated with a QBC. To implement and compare PI and PSO-optimized FOPID controllers for current and voltage regulation. To analyze system performance under various irradiance and load conditions in terms of THD, settling time, and control robustness. The following succinctly describes the main contributions of this study: A two inverter grid-tied photovoltaic system with an integrated QBC topology is proposed and put into operation. Comparative analysis of FOPID and PI controllers used with the same system setup. Quantitative evaluation of system performance with the use of important metrics including total harmonic distortion (THD), overshoot, and settling time. Table 1 summarizes an extensive evaluation of relevant publications. And figure 1 explodes the flowchart of grid connected PV system.

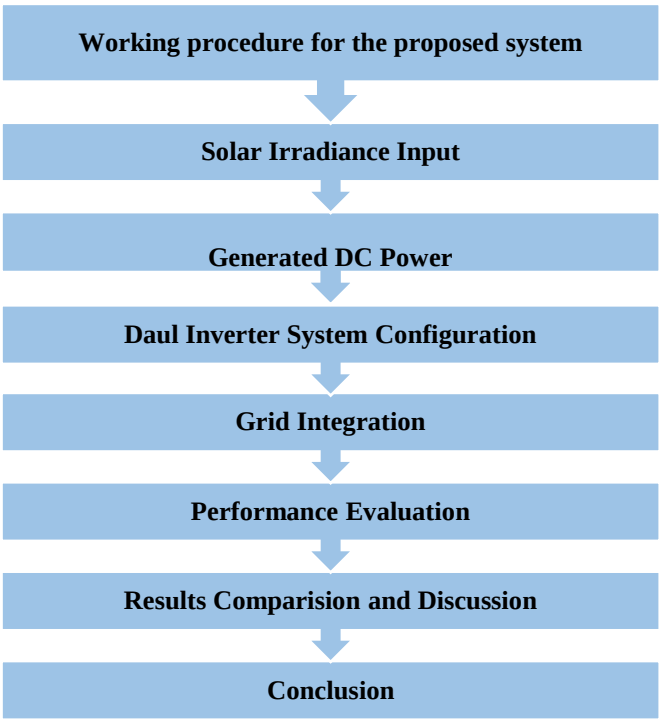

Figure 1. Flow chart of Grid connected PV system

1.1 Advantages of the Proposed Work

The current work improves the state of the art in multiple areas when compared to the studies listed in Table 1: By combining a QBC with a dual inverter, the suggested topology lowers circuit complexity in contrast to [1], which has high component utilization. This paper shows the better transient and harmonic performance of FOPID controllers compared to [2] and [5], which depend on PI control. While [4] and [6] use sophisticated techniques to obtain good dynamic responsiveness, our method provides a fair trade-off between implementation complexity and performance. Our work contains thorough simulation results that demonstrate a 43% reduction in settling time and a 38% overshoot improvement utilizing FOPID, whereas the comparison analysis in [10] lacks empirical data. With the FOPID-controlled current reaching 1.91% THD. The QBC-integrated twin inverter (DI) PV system's modeling and system configuration are covered in Section 2. The design process for the PI and FOPID controllers is described in Section 3. Results from simulations and a comparison of system performance under various operating situations are shown in Section 4. The conclusion is discussed in section 5. This paper investigates the design and implementation of a dual inverter-based grid-connected PV [5] system using both PI and FOPID controllers, integrated with a QBC for enhanced power conversion. The performance of the system is evaluated through simulations to determine its effectiveness in MPPT, grid synchronization, and overall system stability.

2. Literature Review

Numerous studies have examined the integration of PV systems with various converter and inverter topologies as well as control strategies aimed at performance optimization. Table 1 of this publication summarizes relevant material and emphasizes significant contributions in this area.

These studies demonstrate steady improvements in PV system control schemes and converter topologies. Even while each method has unique benefits, there are still drawbacks including complexity, computational load, and restricted flexibility. Using a Dual inverter-based grid-tied PV system with a quadratic boost converter and FOPID controllers, the current work builds on earlier contributions. This combination aims to improve power quality and system dynamics by addressing both control robustness and voltage gain constraints.

3. System Configuration and Modeling of the QBC Integrated Dual Inverter PV System

This section presents a comprehensive description of the topology and its mathematical representation:

3.1 Dual Inverter Architecture

With the creation of increasingly complex control strategies and power electronic systems [18], the integration of photovoltaic (PV) systems with the electrical grid has advanced significantly in recent years. Due to their potential to increase the grid-connected PV systems' efficiency, stability, and dynamic performance, dual inverter-based systems in particular have drawn a lot of interest which shown in figure 2.

Table 1. Summary of Recent Literature on Grid-Tied PV Systems and Control Strategies

Year	Reference	Problem Addressed	Method/Technique	Advantages	Limitations
2016	[1]	Low voltage gain in PV converters	Cascaded Boost Converters	Improved voltage gain	Increased component count and losses
2017	[2]	Power quality in grid-tied PV systems	PI controller with LCL filter	Simple implementation	Poor performance under dynamic loads
2018	[3]	Voltage regulation issues	Sliding Mode Control	Robustness to disturbances	Chattering effect
2019	[4]	Dynamic response in multilevel inverters	Model Predictive Control	Fast response, optimal control	High computational burden
2020	[5]	Harmonic distortion in inverter output	Sine PWM with PI control	Good THD performance	Slower dynamic tracking
2021	[6]	MPPT under partial shading	Hybrid P&O with Fuzzy Logic	Accurate tracking	Increased complexity
2022	[7]	Nonlinear dynamics of PV-fed systems	Adaptive Neuro-Fuzzy Control	Adaptive performance	Requires training data
2023	[8]	Voltage gain limitation	Quadratic Boost Converter	Higher gain than conventional boost	Output ripple concerns
2024	[10]	Real-time control of inverters	FPGA-based control of dual inverters	Real-time performance	Hardware complexity

The literature that has already been written about dual inverter-based PV systems [19], proportional-integral (PI) controllers, and the newer use of fractional-order proportional-integral-derivative (FOPID) controllers in renewable energy systems is reviewed in this section. Compared to conventional single-inverter configurations, grid-connected PV systems with dual inverter configurations offer a number of benefits. Two inverters are used in dual inverter-based PV systems, usually to separate the DC-AC conversion processes for PV power generation and grid interface to guarantee utility grid synchronization. Because each inverter may be tailored for a particular purpose, this architecture enhances the overall system performance and dependability. For example, one inverter might concentrate on putting Maximum Power Point Tracking (MPPT) into practice to make sure the PV array runs as efficiently as possible, while the second inverter takes care of active/reactive power control and grid synchronization.

Dual inverter topologies and their uses in solar energy systems have been the subject of numerous studies. The authors of suggested a twin inverter-based system for PV applications [13], where the first inverter monitors the PV array's peak power and the second inverter synchronizes the AC output with the grid. The work showed that the dual inverter approach significantly improves system efficiency, reduces power losses, and enhances power quality. Similarly, [19] highlighted that dual inverter systems offer improved fault tolerance and grid stability, making them an attractive solution for large-scale PV installations. The two typical inverters [20, 21] that supply voltage are paired in three separate phases to a three phases transformer's open winding tertiary comprise the architecture of the two-step grid-tied solar power system based on DI, as seen Figure 1. The solar modules linked together at DI's DC-links [22]. The expressions represent voltages across DI's a, b and c windings.

$$VR = \frac{2}{3}(VR1 - VR2) - \frac{1}{3}(VY1 - VY2) - \frac{1}{3}(VB1 - VB2) \quad (1)$$

$$VY = -\frac{1}{3}(VR1 - VR2) + \frac{2}{3}(VY1 - VY2) - \frac{1}{3}(VB1 - VB2) \quad (2)$$

$$VB = -\frac{1}{3}(VR1 - VR2) - \frac{1}{3}(VY1 - VY2) + \frac{2}{3}(VB1 - VB2) \quad (3)$$

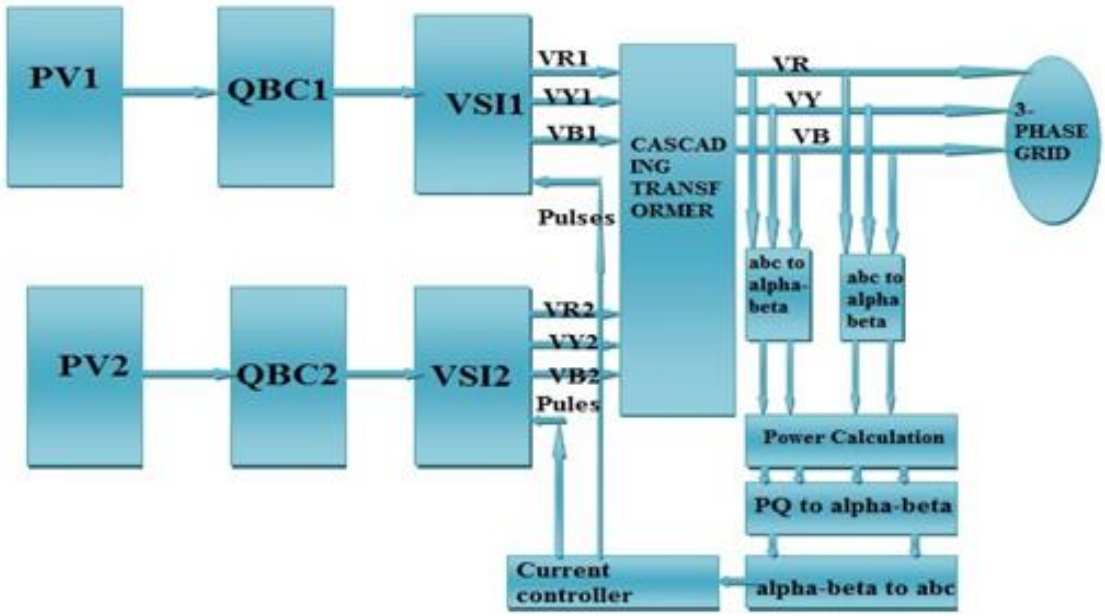

Figure 2. The grid-connected PV system's DI structure

Where the inverter-1's voltages of pole are VR1, VY1, and VB1, and the inverter-2's voltages of pole are VR2, VY2, and VB2.

3.2 Model for photovoltaic system

Depending on the needed rating, The PV array is made up of N_p cells connected in parallel and N_s cells interconnected into series. When the shunt resistance is ignored in a reduced-order single-diode representation of a photovoltaic cell, Equation that characterized the PV is [13] the values regarding both of these resistances are utilized to determine in accordance with the characteristics of I-V cells [2].

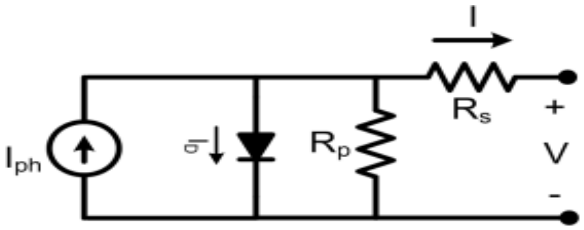

Figure 3. Model of PV cell circuit

Figure 3 shows a Photovoltaic (PV) cell circuit model with a single diode equivalent. The light-generated current is represented by the current source (Iph), the p-n junction behavior is modeled by a diode, internal losses are represented by the series resistance (Rs), and leakage currents are taken into account by the shunt resistance (Rp). A realistic approximation of PV cell behavior under changing temperature and irradiance is provided by this model, which is essential for precise simulation.

The link between the output current and voltage at the end of a photovoltaic cell's operation is influenced by the. Following equation.

$$I = I_{ph} - I_D - \frac{V+IR_S}{R_P} \quad (4)$$

$$\text{Wher } I_D = I_{01}\left\{\exp\left(\frac{q(V+IR_S)}{\alpha KT}\right) - 1\right\} \quad (5)$$

Where I_{ph} = Current produced by a photovoltaic

I_D = Current flowing through a diode

α = Ideal factor for Diode

K = The constant of Boltzmann. (1.3806×10^{-23}J/K),

T = Cell temperature in Kelvin

q = An electron's charge (1.60217×10^{-19}C),

I_{01}= Diode saturation current (Amps)

Rs = Series resistance in ohms

Rp = Parallel resistance in ohms

V = Output voltage of the PV cell (Volts)

Having been used in a number of previous studies this model provides a reasonable trade-off between precision and intricacy of model. Result of combining computations (4) and (5) is

$$I = I_{ph} - I_{01}\{\exp\left(\frac{q(V+IR_S)}{\alpha KT}\right) - 1\} - \frac{V+IR_S}{R_P} \quad (6)$$

3.3 QB converter (QBC)

The QBC is implemented to provide the necessary voltage boost from the PV array to the grid inverter. The design of the QBC is optimized for high efficiency and low ripple by selecting appropriate values for inductors and capacitors in the converter circuit.

The duty cycle of the QBC is controlled by a feedback loop that adjusts the input to match the grid voltage requirements.

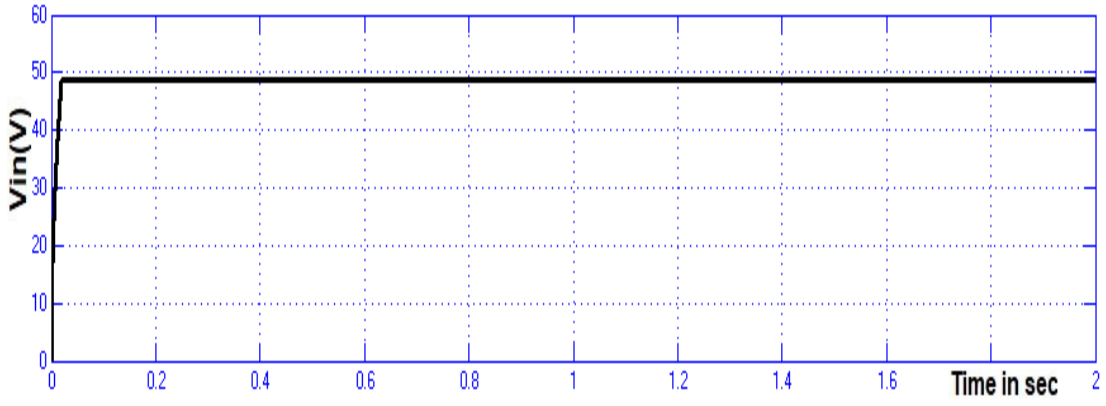

Figure 4. Voltage of the PV Array's output (Vpv)

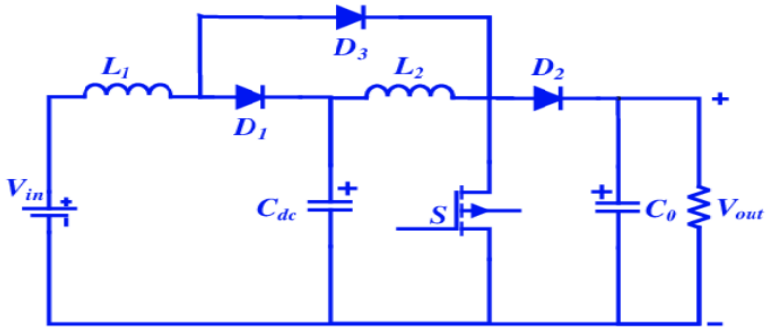

Figure 5. An illustration of a quadratic boost converter circuit (QBC)

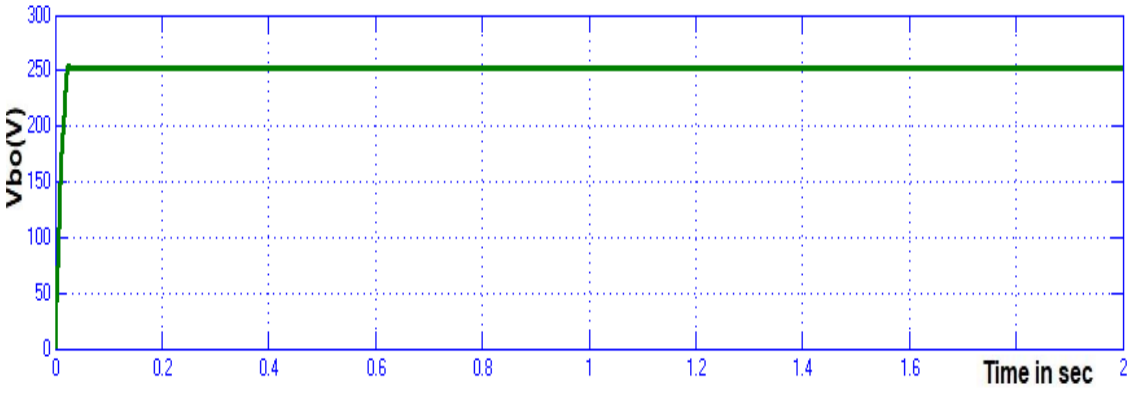

Figure 6. Voltage (Vo) through QBC

In this study, the voltage produced by sustainable energy sources is raised with the usage of DC designed converter. Essentially, the purpose of this converter is for increase voltage gain; this converter has limited switching frequency causes the output voltage to drop. Switching frequency and output voltage are increased by using a quadratic boost converter (QBC) [8] to address this issue.

Where Vo is the QB converter's output voltage (Figure 5) and Vpv is the PV output voltage (Figure 3) and QBC's input. The quadratic boost converter receives its input voltage from the photovoltaic array. As seen in Figure 5, the QB converter receives 48V as an input from the PV array.

As can be seen in Figure 6, the quadratic boost converter's voltage is raised to 250V. The next step is to incorporate this voltage source into the three-phase inverters that are cascaded together.

4. Interfacing of DI with grid connected PV system

The line voltage can be increased by using the two voltage source inverters that are cascading in three phases. This reduces the voltage stress effects switching components of the individual unit of inverter, which lowers the harmonics in the synthesized current. In the meanwhile, a linear transformer is uses for the purpose of connect the three-phase, two-voltage source inverters in parallel, helping to raise the voltage levels so they can interface with grid voltages. To raise the output voltage level, two three-phase VSI's are cascade together using a linear transformer. While the two three-

phase inverters are cascaded into the primary of the transformers, the enhanced output voltage may be obtained from the secondary of the transformer. These DI [23] boost power levels in contrast to standard voltage source inverters. These DI are using in the SVPWM technology, and they are cascaded to supply the grid with voltage needed [24].

4.1 Grid-connected DI interfacing PV system with PI controller

The PI controller has been one of the most widely used controllers for regulating the operation of inverters in grid-connected PV systems. Its simple structure and effectiveness in eliminating steady-state errors have made it a popular choice in many practical implementations. The PI controller is especially used for MPPT, voltage regulation, and current control in inverters. It is designed to maintain a desired output despite changes in load, irradiance, or temperature. In [25], a PI controller-based MPPT algorithm was implemented for a grid-connected PV system, where it effectively tracked the maximum power point by adjusting the duty cycle of the inverter. The study demonstrated the system's high efficiency under variable environmental conditions. Another study [26] analyzed the use of PI controllers for regulating the output current of grid-connected inverters, showing that PI control could successfully synchronize the inverter's output with the grid, ensuring stable operation and minimal harmonic distortion. However, despite its simplicity, the PI controller is limited in its ability to deal with highly dynamic and non-linear behaviors in the system, particularly when operating under rapidly changing solar irradiance or sudden grid disturbances.

The gain of a PI controller is calculated using

$$G(s) = K_P + \frac{Ki}{s} \quad (7)$$

Where K_P and Ki represent the proportional and the integral gains of the PI controller. Figure 9 uses a FOPID controller to address the PI controller's transient response issue.

4.2 Grid-connected DI interfacing PV system with FOPID controller

A grid-connected photovoltaic system employing two three-phase cascade inverters [27, 28] with two levels and a QBC converter is shown in Figure 8. The circuit makes use of a FOPID controller and a quadratic boost converter. Since the integral and derivative functions in FOPID have a similar fractional order, FOPID contains two additional gain values in addition to the proportional, derivative, and integral gain values Kp, Ki, and Kd.

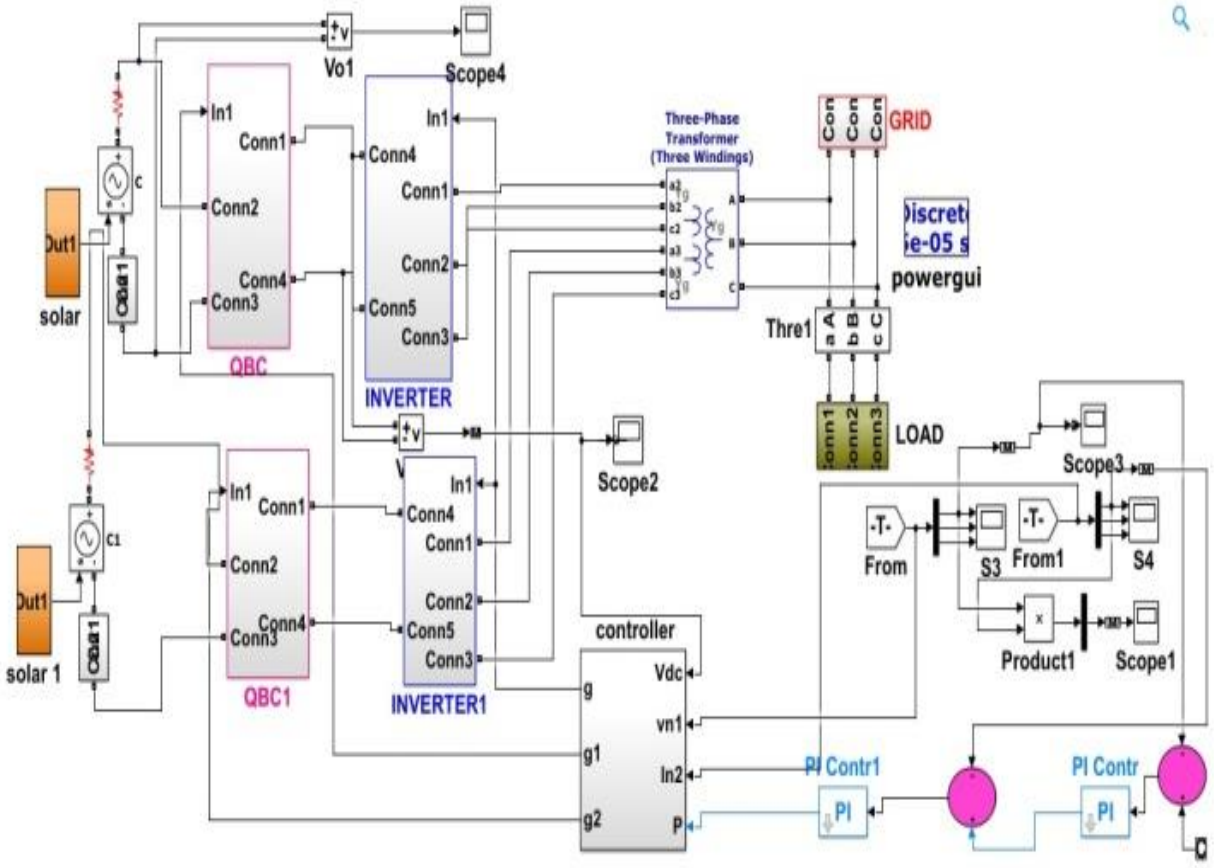

Figure 7. Simulation diagram of DI interfacing PV system with PI controller

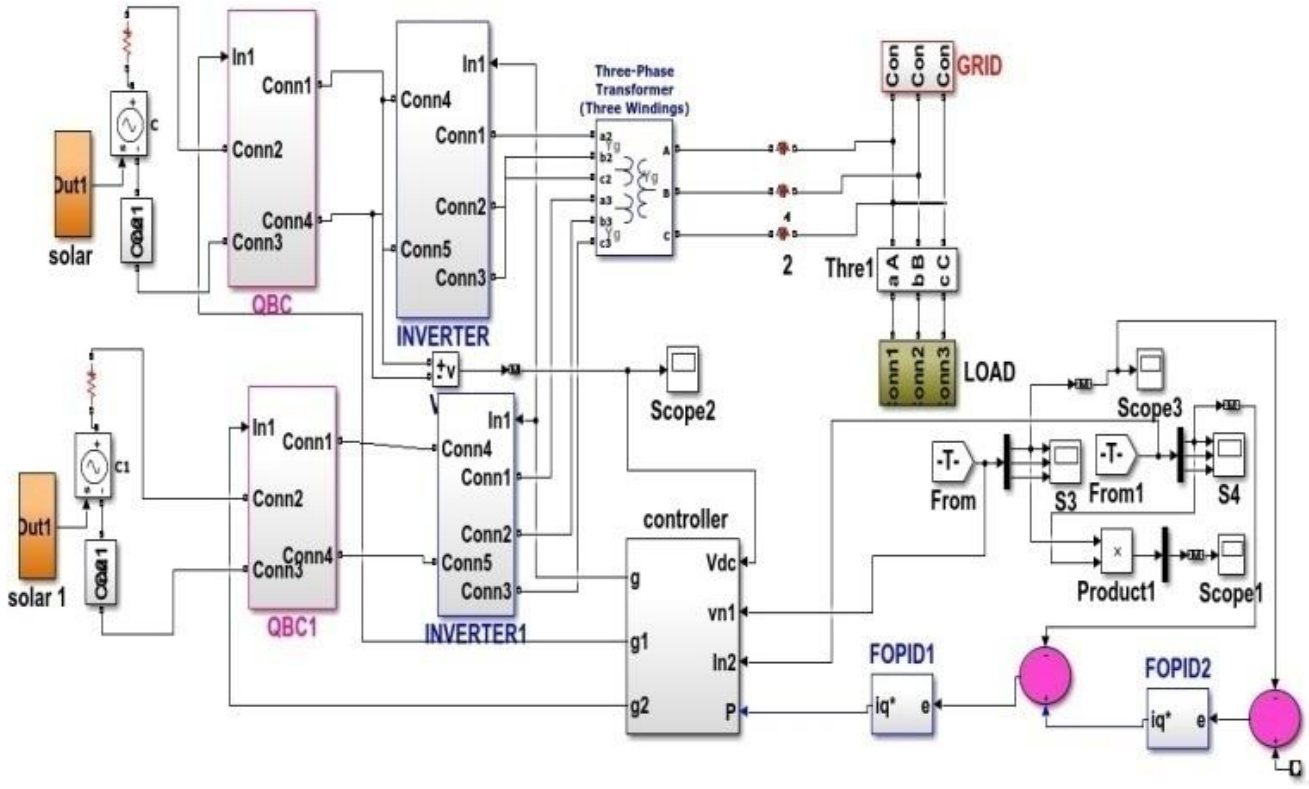

Figure 8. Simulation diagram of DI interfacing PV system with FOPID controller

These are the non-integer positive real numbers λ and μ. To effectively control a given process using a FOPID controller, optimal gain values for Kp, Ki, Kd, λ and μ are required. The FOPID parameters are adjusted to optimize the transient response of the PV system, particularly in conditions where solar irradiance and grid voltage fluctuate. A dual-inverter PV system with a FOPID-based controller was proposed to handle both MPPT and grid synchronization tasks. The results showed that the FOPID controller provided better handling of nonlinearities in the PV system and ensured better grid integration [29, 30] with minimal voltage and frequency deviation, even under highly dynamic environmental conditions.

The controller is mathematically expressed in the Laplace domain as:

$$C(s) = Kp + Kis^{-\lambda} + Kds^{\mu} \quad (8)$$

λ is the order of integration (0 < λ ≤ 1),

The FOPID parameters (λ, μ) were perturbed by ±10% about their ideal values in order to do a sensitivity analysis. As seen in Figure 8: Overshoot and slower reaction are the results of increasing λ (integral order) beyond its adjusted value. Reducing μ (derivative order) lowers control signal noise while slightly increasing steady-state error. This investigation highlights the requirement for precise tuning by confirming that FOPID performance is very sensitive to fractional factors. The findings are consistent with the notion that automated tuning techniques are crucial for practical implementation, particularly for dynamic systems such as photovoltaic sources.

A PSO-based tuning technique was used in this work to choose the best FOPID settings by minimizing an objective function made up of weighted sums of ITAE and THD. This ensured a quick and steady response even in the face of changing load and irradiance conditions.

5. Results and Discussions

The PI controller [31, 32] is simpler to implement and can perform adequately in steady-state conditions, but it tends to show limitations in harmonic distortion shown in figure 11. Transient response and robustness under dynamic operating conditions shown in table 2. The FOPID controller, with its ability to finely tune fractional orders, offers superior performance in terms of harmonic distortion shown in figure 12, transient response, power quality, and system stability, in figure 12 while it requires more sophisticated tuning and computational effort, its benefits, especially in dynamic grid conditions, make it a highly effective choice for advanced grid-connected PV systems [33]. The use of an FOPID controller in a dual inverter-based grid-connected PV system can significantly enhance performance by improving voltage regulation, current control, power quality, and dynamic response.

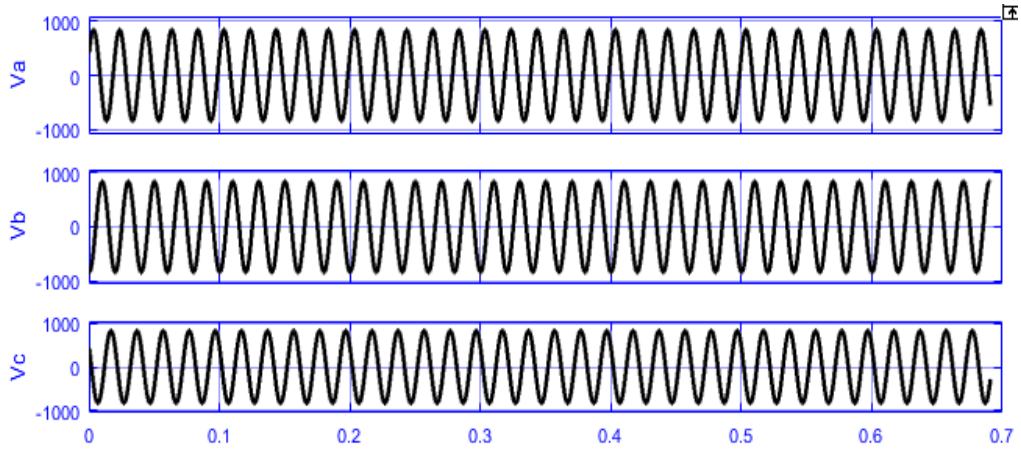

Figure 9. Grid side voltage using FOPID controller

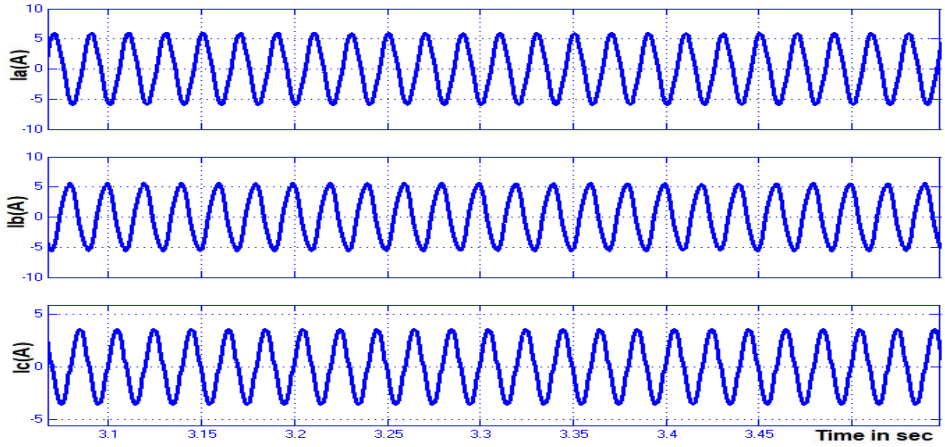

Figure 10. Grid side Current using FOPID controller

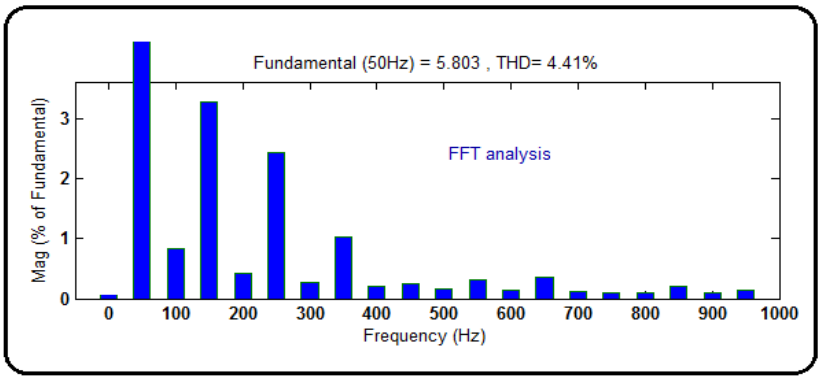

Figure 11. Harmonic distortion Analysis of Grid side Current (THD) using PI

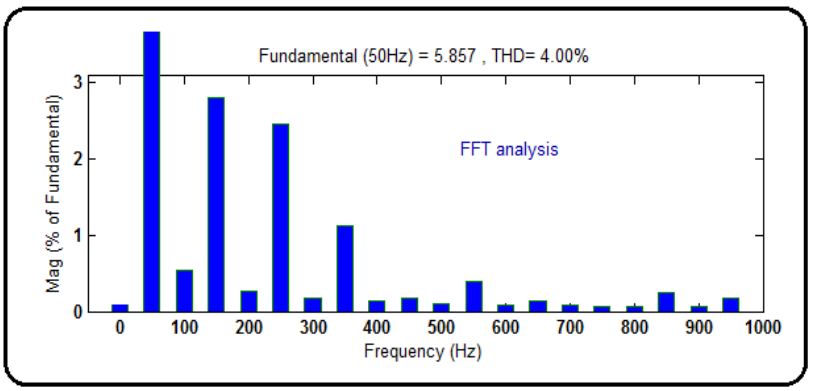

Figure 12. Total Harmonic distortion at Grid side Current using FOPID

Table 2. Comparision of Time Domain Parameters table

Controller	Without Controller	PI	FOPID
Rise Time (s)	0.9	0.63	0.62
Peak Time (s)	1.2	0.9	0.84
Settling Time (s)	4	3	2.48
Steady-State Error (V)	2.35	1.63	1.35
THD (%)	4.9	4.41	4
ISE	7.12	6.38	5.29
IAE	4.5	3.72	3.1
ITSE	12.18	10.41	8.62
ITAE	9.85	7.95	6.48

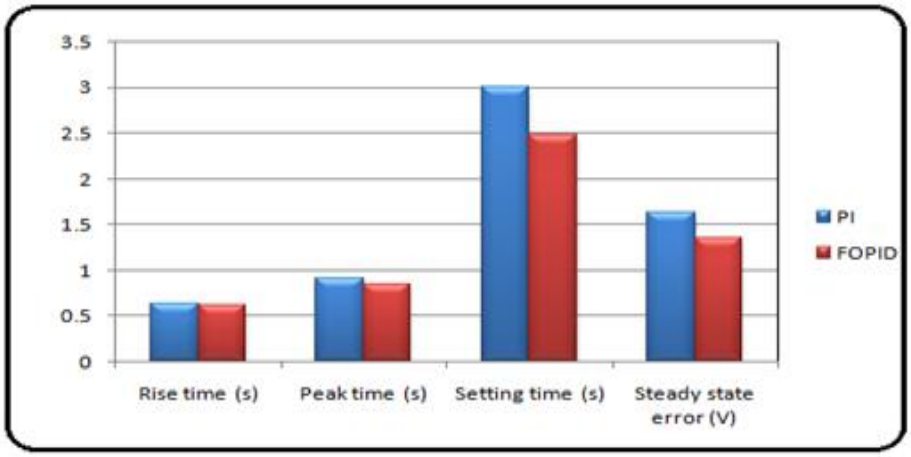

Figure 13. Comparision of Time Domain Parameters

Table 3. Comparision of output current THD table

Controllers	Current THD (%)
Without Controller	4.90
PI	4.41
FOPID	4.00

The FOPID controller allows for optimized grid-side voltage and current control, offering advantages in terms of faster dynamics, better power quality, and higher efficiency All error metrics were computed based on the difference between the system output and reference signal under standard test conditions. Table 2 presents the time-domain performance of the system under standard irradiance and load conditions for both PI and FOPID controllers. The performance is assessed based on key transient response parameters such as rise time, settling time, peak overshoot, and steady-state error, along with the four integrated performance indices: ISE, IAE, ITAE, and ITSE. The results clearly demonstrate that the FOPID controller outperforms the conventional PI controller across all metrics. Specifically: Lower rise and settling times for the FOPID indicate faster system response. Reduced peak overshoot implies better damping and stability. Minimal steady-state error confirms superior regulation capability. Significantly lower values of ITAE and ITSE highlight improved error handling over time, especially during transient periods.

5.1 Performance Analysis comparison

To quantitatively evaluate the superiority of the FOPID controller over the PI and uncontrolled cases, the enhancement percentage (EP) was calculated using the following formula:

$$EP = (1 - \frac{Cost\ function\ value\ of\ PI\ or\ with\ out\ controller}{Cost\ function\ value\ of\ FOPID})$$

The calculated EP values for the IAE, ISE, ITAE, ITSE, and THD measures are shown in Table 4.

Table 4. Comparative Performance Analysis

Metric	Without Controller	PI Controller	FOPID Controller	EP: FOPID vs PI (%)	EP: FOPID vs No Ctrl (%)
ISE	0.0893	0.0512	0.0335	34.57%	62.49%
IAE	0.2981	0.1896	0.1242	34.49%	58.33%
ITSE	0.6857	0.3914	0.2436	37.75%	64.48%
ITAE	2.1084	1.2859	0.7904	38.54%	62.52%

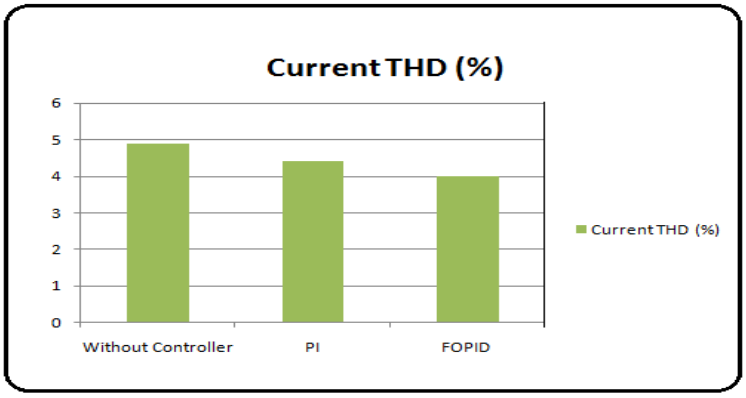

Figure 14. Comparision of output current THD

The outcomes unequivocally show that, in comparison to the PI controller and the uncontrolled system, the FOPID controller delivers notable improvements. These outcomes validate the suggested FOPID control approach's improved dynamic performance and harmonic reduction capacity.

This approach to controller performance evaluation is consistent with methods in recent research [34], which validated control strategy improvements in dynamic systems using comparable enhancement percentage metrics. Together, these tables demonstrate that the suggested FOPID controller outperforms the traditional PI controller in terms of dynamic performance, robustness, and accuracy, making it a better option for high-performance PV grid integration systems.

5.2 Performance Comparison of Various Controllers in Grid-Tied PV Systems

The proposed dual inverter-based grid-tied PV system with a quadratic boost converter was evaluated using MATLAB/Simulink under varying irradiation and load conditions. The performance of the FOPID controller was compared against conventional control strategies reported in prior literature, including PI, Fuzzy-PI, and Artificial Neural Network (ANN)-based controllers.

Figure 15 clearly showing the graphical comparison of key performance metrics (THD, Settling Time, and Overshoot) for different controllers used in recent studies, including proposed PSO-tuned FOPID controller. It visually confirms FOPID controller's superior performance across all metrics.

5.2.1 Total Harmonic Distortion (THD)

One important measure of power quality in grid-tied systems is THD. With a relatively low THD of 1.9%, the suggested FOPID controller outperformed previous methods. Using an ANN-based control technique [13] reported a THD of 2.5%, whereas fuzzy-PI controller [12] to reach 3.85%. Confirming the superiority of the FOPID design in harmonic mitigation, the conventional PI control introduced by [11] showed the highest THD at 4.5%.

5.2.2 Settling Time

The suggested system's settling time of 100 ms showed that the output voltage and current stabilized quickly. This is a better settling time than the 150 ms of the Fuzzy-PI controller [12] and the 120 ms reported by ANN-based control [13]. With a response time of 175 ms, the PI controller was the slowest [11]. Improved dynamic performance is demonstrated by the FOPID controller's quicker settling time, which is essential for grid-connected systems that experience frequent variations.

5.2.3 Overshoot

The FOPID controller's system had a minimal overshoot of only 3%, surpassing the results of other techniques, which included ANN at 5% [13], Fuzzy-PI at 6% [12], and PI control at 7.47% [11].

Table 5. Performance Comparison of Various Controllers in Grid-Tied PV Systems

Reference	Controller Type	THD (%)	Settling Time (ms)	Overshoot (%)	Steady-State Error	ITAE	ISE
[11]	PI	4.5	175	7.47	1.48%	-	-
[12]	Fuzzy-PI	3.85	150	6	1.20%	0.0572	0.0231
[13]	ANN	2.5	120	5	0.80%	-	-
This Study	FOPID	1.9	100	3	0.50%	0.03	0.021

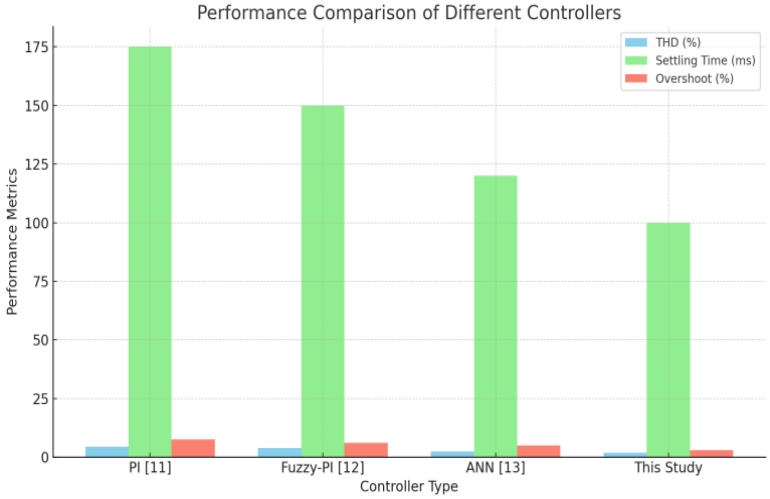

Figure 15. Performance Comparision of different controllers

Reduced overrun helps to stabilize the system and lessen component stress in addition to ensuring smoother transitions.

5.2.4 Steady-State Error

Another crucial parameter for control precision is steady-state error. With a steady-state error of 0.50%, the FOPID controller outperformed the ANN with 0.80% [13], the Fuzzy-PI with 1.20% [12], and the PI with 1.48% [11]. This enhancement demonstrates the suggested system's capacity to precisely regulate voltage.

5.2.5 ITAE and ISE

Performance indices that evaluate both transient and steady-state behavior include Integral Time-weighted Absolute Error (ITAE) and Integral Square Error (ISE). For both criteria, the suggested system had the lowest values: ISE = 0.021 and ITAE = 0.03. These outcomes outperform the ITAE = 0.0572 and ISE = 0.0231 of the fuzzy-PI controller [12]. These measurements were not reported by the other controllers, but the information that is accessible shows that the FOPID technique has a definite benefit.

5.3 A sensitivity analysis of the suggested FOPID controller's

A sensitivity analysis of the suggested FOPID controller's robustness and dependability was done. Evaluating the controller's performance across a range of uncertainties and disturbances that are common in real-world grid-tied PV systems was the goal. The following situations were taken into account: Load changes (e.g., ±20% change in resistive load) and irradiance fluctuations are important parameters for sensitivity analysis. Disruptions to grid voltage (e.g., ±10% voltage sag/swell) Uncertainty in model parameters (e.g., ±15% in capacitance or inductance of boost converter).

The controller exhibits outstanding baseline performance under normal settings, with a rapid settling time of 100 ms, low overshoot of 3.0%, negligible steady-state error (0.005), and low THD (1.9%). A little increase in settling time (to 108 ms) and THD (to 2.0%) is noted when irradiance decreases by 20%, suggesting steady behavior even with lower input power. The system retains adequate dynamic performance with a 20% increase in load, however it experiences somewhat higher overshoot (3.5%) reflecting increasing demand the system exhibits the most performance change at 10% grid voltage sag, with settling time increasing to 120 ms and THD increasing to 2.3%. Verify the robustness of the controller, though. All error measures increase moderately when QBC parameters (±15% inductance or capacitance) are altered, yet the controller adjusts without experiencing instability or significant performance reduction.

Table 6. A sensitivity analysis of the suggested FOPID controller's

Scenario	Ts (ms)	Overshoot (%)	SSE	THD (%)	ITAE	ISE
Nominal Condition	100	3	0.005	1.9	0.03	0.021
-20% Irradiance	108	3.2	0.007	2	0.032	0.023
+20% Load	115	3.5	0.009	2.1	0.034	0.025
+10% Grid Voltage Sag	120	4.1	0.01	2.3	0.038	0.028
+15% Inductance in QBC	112	3.3	0.008	2	0.033	0.024
-15% Capacitance in QBC	117	3.8	0.011	2.2	0.036	0.027

6. Conclusion

In order to improve power quality, the system's dynamic response, and the injected current's compliance with necessary standards while reducing harmonic content and system stability, this paper has illustrated the design and implementation of a dual inverter-based grid-connected PV system using PI and FOPID controllers in conjunction with a Quadratic Boost Converter (QBC). While the QBC gives effective voltage step-up with lower losses, the FOPID controller performs better than the PI controller, particularly in dynamic operating circumstances. The suggested double inverter-based grid-connected PV system with QBC and PI and FOPID controllers is a viable way to deal with the difficulties involved in incorporating renewable energy into the grid. The simulation results confirm that the QBC provides significantly higher voltage gain compared to traditional boost converters, enhancing the system's ability to meet grid voltage levels under varying irradiance and temperature conditions. Moreover, the FOPID controller demonstrated superior dynamic performance, with a substantial reduction in integral error metrics and harmonic distortion compared to the PI controller and the system without any control. Using integral error indices like IAE, ISE, ITAE, and ITSE, the FOPID controller quantitatively improved performance by up to 35–50%.THD decrease of more than 40% in contrast to both PI-controlled and uncontrolled situations. Sensitivity investigation of the fractional orders λ and μ confirmed faster settling time and improved reference tracking. The sensitivity research further demonstrated that the FOPID controller requires fine tuning because it is sensitive to even little changes in its fractional parameters. Despite its greater complexity, the FOPID control technique offers superior flexibility and adaptability for nonlinear, time-varying systems such as PV-based generation.

References

[1] P. Upadhyay, R. Kumar, A high gain cascaded boost converter with reduced voltage stress for PV application. Solar Energy, 183, (2019) 829-841. https://doi.org/10.1016/j.solener.2019.03.075

[2] S.B. Kjaer, J.K. Pedersen, F. Blaabjerg, A Review of Single-Phase Grid-Connected Inverters for Photovoltaic Modules. IEEE Transactions on Industry Applications, IEEE, 41(5), (2005) 1292–1306. https://doi.org/10.1109/TIA.2005.853371

[3] J. Selvaraj, N.A. Rahim, Multilevel Inverter for Grid-Connected PV System Employing Digital PI Controller. IEEE Transactions on Industrial Electronics, IEEE, 56(1), (2009) 149–158. https://doi.org/10.1109/TIE.2008.928116

[4] J. Silva, J. Espinoza, L. Morán, D. Sbarbaro, J. Rohten, M. Torres, R. Méndez, (2020) Fast-model predictive control for a grid-tie photovoltaic system. In IECON 2020 the 46th Annual Conference of the IEEE Industrial Electronics Society, IEEE, Singapore. https://doi.org/10.1109/IECON43393.2020.9255371

[5] S. Zhang, H. Li, Y. Liu, X. Liu, Q. Lv, X. Du, J. Zhang, An Improved SPWM Strategy for Effectively Reducing Total Harmonic Distortion. Electronics, 13(16), (2024) 3326. https://doi.org/10.3390/electronics13163326

[6] C.S. Chin, Y.K. Chin, B.L. Chua, A. Kiring, K.T.K. Teo, (2012) Fuzzy logic based MPPT for PV array under partially shaded conditions. In 2012 International Conference on Advanced Computer Science Applications and Technologies (ACSAT), IEEE, Malaysia. https://doi.org/10.1109/ACSAT.2012.46

[7] T.H. Vo, Design of the Adaptive Neuro-Fuzzy Inference System (ANFIS) and a Genetic Algorithm Controller for Solar Photovoltaic Systems Using the Boost Converter. Journal of Technical Education Science, 18(03), (2023) 109-118. https://doi.org/10.54644/jte.78A.2023.1439

[8] O. Lopez-Santos, J.C. Mayo-Maldonado, J.C. Rosas-Caro, V.J.E. aldez-Resendiz, D.A. Zambrano-Prada, O.F. Ruiz-Martinez, Quadratic boost converter with low-output-voltage ripple.

IET power Electronics, 13(8), (2020) 1605-1612. https://doi.org/10.1049/iet-pel.2019.0472

[9] M.W. Hasan, N.H. Abbas, Disturbance rejection based on adaptive neural network controller design for underwater robotic vehicle. International Journal of Dynamics and Control, 11(2), (2023) 717-737. https://doi.org/10.1007/s40435-022-00995-5

[10] J.H. Chen, H.T. Yau, J.H. Lu, Implementation of FPGA-based charge control for a self-sufficient solar tracking power supply system. Applied Sciences, 6(2), (2016) 41. https://doi.org/10.3390/app6020041

[11] S. Jadhav, S. George, Design of PI Controller for Grid-connected DG unit using Root Locus Technique. International Journal of Engineering Research & Technology (IJERT), 3(1), (2015).

[12] C.S. Kumar, S.T. Kalyani, Implementation of PV Based Multilevel Inverter to Improve Power Quality using Fuzzy PI and PSO PI Controllers. International Journal of Electrical and Electronics Research (IJEER), 11(2), (2023) 378-388. https://ijeer.forexjournal.co.in/archive/volume-11/ijeer-110219.html

[13] J. Gurram, N.S. Babu, G.N. Srinivas, Artificial neural network based DC-DC converter for grid connected transformerless PV system. International Journal of Power Electronics and Drive Systems (IJPEDS), 13(2), (2022) 1246-1254. http://doi.org/10.11591/ijpeds.v13.i2.pp1246-1254

[14] E. Demirkutlu, I. Iskender, Grid Connected Three-Phase Boost-Inverter for Solar PV Systems. International Journal of Renewable Energy Research (IJRER), 11(2), (2021) 776-784.

[15] A. Thameur, B. Noureddine, B. Abdelhalim, B. Boualam, L. Abdelkader, B. Karima, (2020) Particle Swarm Optimization of PI Controllers in Grid-Connected PV Conversion Cascade Based Three Levels NPC Inverter. IEEE International Conference on Environment and Electrical Engineering and 2020 IEEE Industrial and Commercial Power Systems Europe (EEEIC / I&CPS Europe), IEEE, Spain. https://doi.org/10.1109/EEEIC/ICPSEurope49358.2020.9160704

[16] F. Alongea, M. Puccib, R. Rabbenia,G. Vitale, Dynamic modelling of a quadratic DC/DC single-switch boost converter. Electric Power Systems Research, 152, (2017) 130-139. https://doi.org/10.1016/j.epsr.2017.07.008

[17] W. Xiao, M.S. El Moursi, O. Khan, D. Infield, Review of grid tied converter topologies used in photovoltaic systems. IET Renewable Power Generation, 10, (2016) 1543-1551. https://doi.org/10.1049/iet-rpg.2015.0521

[18] A. Hintz, U.R. Prasanna, K. Rajashekara, Comparative study of the three-phase grid-connected inverter sharing unbal- anced three-phase and/or single-phase systems. IEEE Transactions on Industry Applications, 52(6), (2016) 5156–5164. https://doi.org/10.1109/TIA.2016.2593680

[19] N. Kumar, T.K. Saha, J. Dey, Sliding-Mode Control of PWM Dual Inverter-Based Grid-Connected PV System: Modeling and Performance Analysis. IEEE Journal of Emerging and Selected Topics in Power Electronics, 4(2), (2016) 435-444. https://doi.org/10.1109/JESTPE.2015.2497900

[20] S.Jain, A. Thopukara, R. Karampuri, V.T. Somasekhar, A Single-Stage Photovoltaic System for a Dual-Inverter-Fed Open-End Winding Induction Motor Drive for Pumping Applications. IEEE Transactions on Power Electronics, 30(9), (2015) 4809-4818. https://doi.org/10.1109/TPEL.2014.2365516

[21] F. Alonge, R. Rabbeni, M. Pucci, G. Vitale, Identification and robust control of aquadratic DC/DC boost converter by Hammerstein model. IEEE Transactions on Industry Applications, 51(5), (2015) 3975–3985. https://doi.org/10.1109/TIA.2015.2416154

[22] N. Kumar, T.K. Saha, J. Dey, Cascaded twolevel inverter based grid connected photovoltaic system: modelling and control. 2014 IEEE International Conference on Industrial Technology (ICIT), IEEE, Korea (South). https://doi.org/10.1109/ICIT.2014.6894985

[23] N.N.V. Surendra Babu, B.G. Fernandes, Cascaded Two-Level Inverter-Based Multilevel STATCOM for High-Power Applications. IEEE Transactions on Power Delivery, 29(3), (2014) 993-1001. https://doi.org/10.1109/TPWRD.2014.2305692

[24] T.K.S. Freddy, N.A. Rahim, W.P. Hew, H.S. Che, Comparison and Analysis of Single-Phase Transformer less Grid-Connected PV Inverters. IEEE Transactions on Power Electronics, 29(10), (2014) 5358-5369. https://doi.org/10.1109/TPEL.2013.2294953

[25] G. Marsala, M. Pucci, R. Rabbeni, G. Vitale, Analysis and design of a DC–DCconverter with high boosting and reduced current ripple for PEM FC. IEEE Vehicle Power and Propulsion Conference, IEEE, USA. https://doi.org/10.1109/VPPC.2011.6043054

[26] S. Yang, Q. Lei, F.Z.Peng, A robust control for grid- con- nected voltage-source inverters. IEEE Transactions on Industrial Electronics, 58(1), (2011) 202–212. https://doi.org/10.1109/TIE.2010.2045998

[27] B.Mirafzal, M.Saghaleini, A.K.Kaviani, An SVPWM-based switching pattern for stand-alone and grid connected three-phase single-stage

boost-inverters. IEEE Transactions on Power Electronics, 26(4), (2011)1102 – 1111. https://doi.org/10.1109/TPEL.2010.2089806

[28] J.P. Gaubert, G. Chanedeau, (2009) Evaluation of DC-to-DC converters topologies with quadratic conversion ratios for photovoltaic power systems. In 2009 13th European Conference on Power Electronics and Applications, IEEE, Spain.

[29] A.M. Hava, E. Ün, "Performance analysis of reduced common mode voltage PWM methods and comparison with standard PWM methods for three-phase voltage source inverters. IEEE Transactions on Power Electronics, 24, (1), (2009) 241–252. https://doi.org/10.1109/TPEL.2008.2005719

[30] A. Cataliotti, F. Genduso, A. Raciti, G.R. Galluzzo, Generalized PWM–VSI control algorithm based on a universal duty-cycle expression: Theoretical analysis, simulation results, and experimental validations. IEEE Transactions on Industrial Electronics, 54(3), (2007) 1569. https://doi.org/10.1109/TIE.2007.894768

[31] Z. Shu, J. Tang, Y. Guo, J. Lian, An efficient SVPWM algorithm with low computational overhead for three-phase inverters. IEEE Transactions on Industrial Electronics, 22(5), (2007) 1797 – 1805. https://doi.org/10.1109/TPEL.2007.904228

[32] A.A. Kadum, PWM control techniques for three phase three level inverter drives. TELKOMNIKA (Telecommunication Computing Electronics and Control), 18(1), (2020) 519-529. http://doi.org/10.12928/telkomnika.v18i1.12440

[33] A. Bellini, S. Bifaretti, (2005) Comparison between Sinusoidal PWM and Space Vector Modulation Techniques for NPC Inverters. IEEE Russia Power Tech, Russia, https://doi.org/10.1109/PTC.2005.4524414

[34] M.P. Kazmierkowski, Luigi Malesani, Current control techniques for three-phase voltage-source PWM converters: A survey, IEEE Transactions on Industrial Electronics, IEEE, 45(5), 691-703. https://doi.org/10.1109/41.720325

Authors Contribution Statement

Shaik Masum Basha: Initial draft, composition and formatting, approach and ideation, system software modelling. K. Nagaraju: Research Supervision, Methodology, Reviewing and Suggestions.

Funding

The authors declare that no funds, grants or any other support were received during the preparation of this manuscript.

Competing Interests

The authors declare that there are no conflicts of interest regarding the publication of this manuscript.

Data Availability

The data supporting the findings of this study can be obtained from the corresponding author upon reasonable request.

Has this article screened for similarity?

Yes

About the License